

Performance of the Gas-jet Transport System Coupled to the RIKEN Gas-filled Recoil Ion Separator GARIS for the $^{238}\text{U}(^{22}\text{Ne}, 5\text{n})^{255}\text{No}$ Reaction

H. Haba,^{a,*} H. Kikunaga,^{a,b} D. Kaji,^a T. Akiyama,^{a,c} K. Morimoto,^a K. Morita,^a T. Nanri,^d K. Ooe,^b N. Sato,^{a,c} A. Shinohara,^b D. Suzuki,^d T. Takabe,^b I. Yamazaki,^d A. Yokoyama,^d and A. Yoneda^a

^aNishina Center for Accelerator Based Science, RIKEN, Wako, Saitama 351-0198, Japan

^bGraduate School of Science, Osaka University, Toyonaka, Osaka 560-0043, Japan

^cDepartment of Physics, Saitama University, Sakura, Saitama 338-8570, Japan

^dFaculty of Science, Kanazawa University, Kanazawa, Ishikawa 920-1192, Japan

^eDepartment of Physics, Tohoku University, Aoba, Sendai 980-8578, Japan

Received: May 1, 2008; In Final Form: June 27, 2008

The performance of the gas-jet transport system coupled to the RIKEN gas-filled recoil ion separator GARIS was investigated using ^{255}No produced in the $^{238}\text{U}(^{22}\text{Ne}, 5\text{n})^{255}\text{No}$ reaction. Alpha particles of ^{255}No separated with GARIS and transported by the gas-jet system were measured with a rotating wheel apparatus for α spectrometry under low background condition. The high gas-jet efficiencies of about 75% were independent of the recoil ranges of ^{255}No in the gas-jet chamber. The present results suggest that the GARIS/gas-jet system is a promising tool for the next-generation superheavy element chemistry: (i) the background radioactivities of unwanted reaction products are strongly suppressed, (ii) the intense beam is absent in the gas-jet chamber and hence the high gas-jet efficiency is achieved, and (iii) the beam-free condition also allows for investigations of new chemical systems

1. Introduction

Chemical studies of superheavy elements (SHEs) with atomic numbers $Z \geq 104$ have become one of the most exciting and challenging research subjects in nuclear and radiochemistry.^{1,2} The extremely low production yields and short half-lives of SHEs force us to conduct rapid and efficient on-line chemical experiments with “single atoms”. Using a gas-jet transport technique, the experimental studies on the chemical properties of SHEs have been performed for elements 104 (Rf) to 108 (Hs) and recently element 112.¹⁻³ At the same time, many of these successful experiments have clearly demonstrated the limitations of the applied techniques. Large amounts of background radioactivities from unwanted reaction products become unavoidable with increasing Z of SHEs of interest. High-intensity beams from advanced heavy-ion accelerators also give rise to a problem in that the plasma formed by the beam in the target chamber significantly reduces the gas-jet transport efficiency. To overcome these limitations, the concept of physical preseparation of SHE atoms has been proposed.^{1,4} With this method, background radioactivities originating from unwanted reaction products are largely removed. The high and stable gas-jet efficiencies are achieved owing to the condition free from plasma. Furthermore, this beam-free condition allows us investigations of new chemical systems that were not accessible before.⁴ The pioneering experiments with the recoil transfer chamber (RTC) coupled to the Berkeley Gas-filled Separator (BGS) were very successful.^{5,6} The isotope of ^{257}Rf physically separated from the large amount of β -decaying products was identified with a liquid scintillator after a liquid-liquid solvent extraction. Thereafter, the BGS/RTC system was used in the model experiments of Rf⁷⁻⁹ and Hs.¹⁰ At Gesellschaft für Schwerionenforschung (GSI), a new gas-filled separator, the TransActinide Separator and Chemistry Apparatus (TASCA), is under commissioning

as a preseparator for chemical studies.^{4,11}

In the RIKEN Linear Accelerator (RILAC) facility, a gas-jet transport system was installed at the focal plane of the RIKEN gas-filled recoil ion separator GARIS to start the SHE chemistry.¹² The performance of the system was first appraised using ^{206}Fr and ^{245}Fm produced in the $^{169}\text{Tm}(^{40}\text{Ar}, 3\text{n})^{206}\text{Fr}$ and $^{208}\text{Pb}(^{40}\text{Ar}, 3\text{n})^{245}\text{Fm}$ reactions, respectively.¹² Alpha particles of ^{206}Fr and ^{245}Fm separated with GARIS and transported by the gas-jet system were measured with a rotating wheel apparatus for α spectrometry under low background condition. The high gas-jet efficiencies of over 80% were found to be independent of the beam intensity up to 2 particle μA (μA).

In order to produce SHE nuclides with long half-lives for chemical experiments, further asymmetric fusion reactions based on actinide targets such as ^{238}U , ^{244}Pu , and ^{248}Cm should be considered (hot fusion reactions). However, very small recoil velocities of evaporation residues (ERs) produced by such asymmetric reactions cause serious problems in the operation of a gas-jet system coupled to a gas-filled separator. The transport efficiency of the gas-filled separator drastically decreases with decreasing recoil velocity due to the multiple small-angle scattering in the filling gas. A vacuum window foil, which separates the gas-jet chamber from the gas-filled separator, should be thin enough ($\approx 1 \mu\text{m}$ as Mylar) to allow ERs to pass through and has to withstand a pressure difference of about 100 kPa. In this work, the performance of the GARIS/gas-jet system for the hot fusion reactions was investigated for the first time using ^{255}No produced in the $^{238}\text{U}(^{22}\text{Ne}, 5\text{n})^{255}\text{No}$ reaction. The ^{255}No atoms pre-separated with GARIS were successfully extracted by the gas-jet system to a distant site where the rotating wheel apparatus for α spectrometry was equipped. The setting parameters such as the magnetic field of the separator and the gas-jet conditions were optimized to obtain the highest yield of ^{255}No .

*Corresponding author: haba@riken.jp

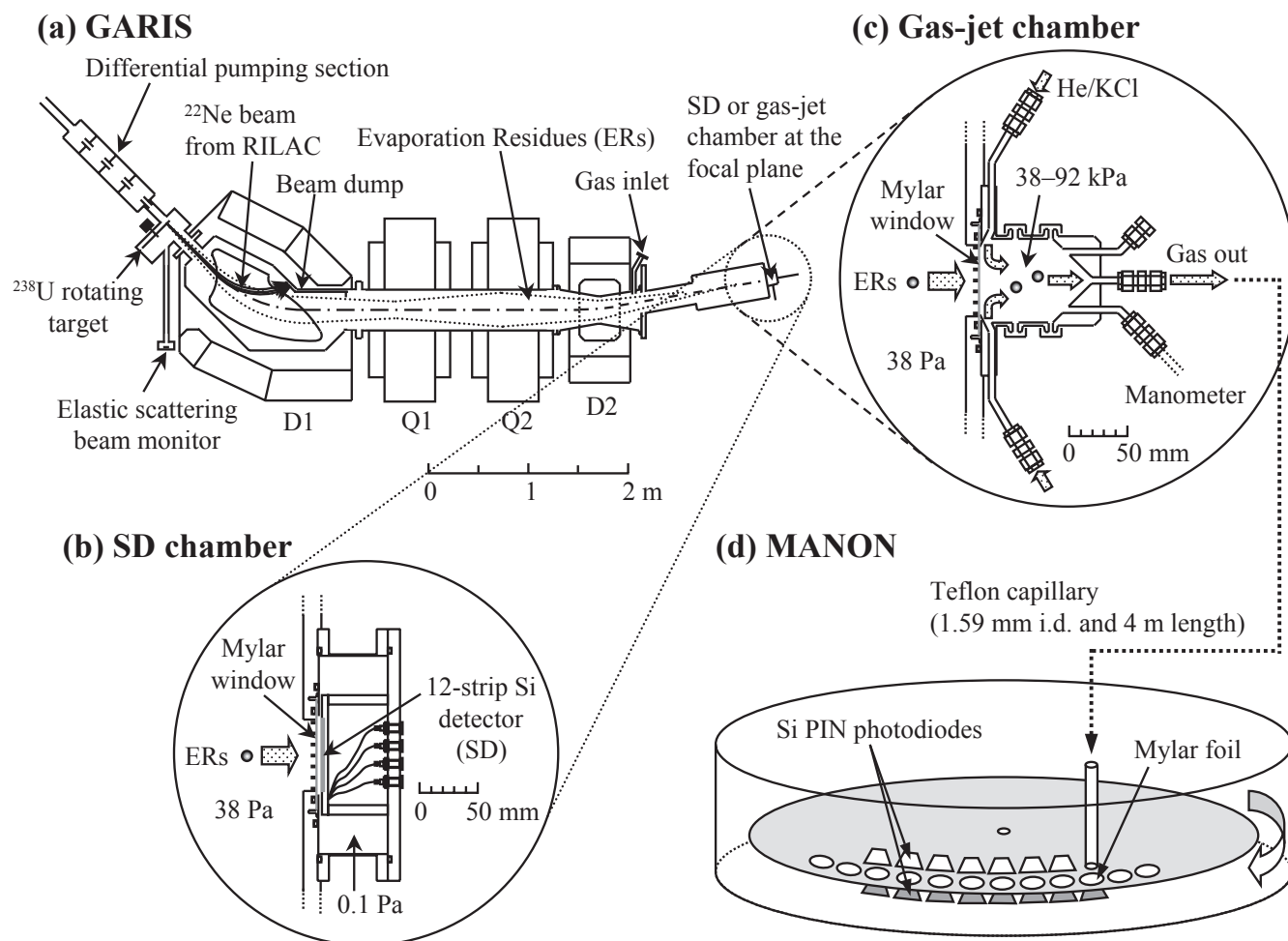


Figure 1. A schematic of the experimental setup: (a) RIKEN gas-filled recoil ion separator GARIS; (b) 12-strip Si detector (SD) chamber; (c) Gas-jet chamber; (d) Rotating wheel apparatus MANON for α spectrometry.

2. Experimental

A schematic of the experimental setup is shown in Figure 1. The $^{22}\text{Ne}^{7+}$ ion beam was extracted from RILAC. A $^{238}\text{U}_3\text{O}_8$ target of $370 \mu\text{g cm}^{-2}$ thickness was prepared by electrodeposition in 2-propanol onto a 1.27 mg cm^{-2} titanium backing foil. The details of the target preparation are reported elsewhere.¹³ Sixteen targets were mounted on a rotating wheel of 30 cm in diameter. The wheel was rotated during the irradiation at 3000 rpm. The beam energy was 113.8 MeV at the middle of the target. At this incident energy, the excitation function for the $^{238}\text{U}(^{22}\text{Ne}, 5n)^{255}\text{No}$ reaction exhibits the maximum cross section of 90 nb.¹⁴ The beam intensity was monitored by measuring elastically scattered projectiles with a Si PIN photodiode (Hamamatsu S1223) mounted at 45° with respect to the beam axis. The typical beam intensity was $4 \mu\text{A}$. GARIS was filled with helium at a pressure of 37 Pa. The other details of GARIS are given elsewhere.¹⁵

As shown in Figures 1a and 1b, the evaporation residues of interest were separated in-flight from beam particles and transfer reaction products with GARIS, and were implanted into a 12-strip Si detector (SD) of $60 \times 60 \text{ mm}^2$ (Hamamatsu 12CH PSD) through a Mylar window foil which was supported with a circular-hole (4.0 mm diameter) grid with 71.6% transparency and of 60 mm diameter. The thickness of the Mylar foil was determined to be $1.1 \pm 0.1 \mu\text{m}$ based on the energy loss of 5.486-MeV α particles from ^{241}Am and on the stopping powers calculated with the SRIM code.¹⁶ The cycle of the beam-on (300 s) and beam-off (600 s) measurements was performed, because no α peaks of ^{255}No were observed in the beam-on spectrum due to large amounts of background events. The α -particle

energy resolutions of the 12 SDs were 20–60 keV FWHM. All events were registered in an event-by-event mode using the VME LIST/PHA module (Iwatsu A3100). The magnetic rigidities of 1.73, 1.82, 1.93, and 2.04 T m were examined to optimize the transport efficiency of GARIS for ^{255}No .

In the gas-jet transport experiments, the reaction products separated with GARIS were guided into the stainless-steel gas-jet chamber of 60 mm depth as shown in Figure 1c. The magnetic rigidity was set at 1.93 T m. The ^{255}No atoms were stopped in the helium gas, attached to aerosol particles generated by sublimation of the KCl powder, and were continuously transported through a Teflon capillary (1.59 mm i.d., 4 m length) to the rotating wheel apparatus MANON for α spectrometry (Figure 1d) which was the compact one of the Measurement system for the Alpha-particle and spontaneous fission events ON-line developed at Japan Atomic Energy Agency (JAEA).¹⁷ The temperature of the KCl aerosol generator was fixed to 620°C based on the previous $^{169}\text{Tm}(^{40}\text{Ar}, 3n)^{206}\text{Fr}$ experiment.¹² The flow rates of the helium gas were varied at 1.0, 2.0, 3.0, 4.0, and 5.0 L min^{-1} , which resulted in the inner pressures of the gas-jet chamber of 38, 54, 69, 81, and 92 kPa, respectively. In MANON, the aerosol particles were deposited on 200-position Mylar foils of $0.68 \mu\text{m}$ thickness placed at the periphery of a stainless steel wheel of 420 mm diameter. The wheel was stepped at 90-s interval to position the foils between seven pairs of Si PIN photodiodes (Hamamatsu S3204-09). Each detector had an active area of $18 \times 18 \text{ mm}^2$ and a 38% counting efficiency for α particles. The α -particle energy resolution was 60 keV FWHM for the detectors which look at the sample from the collection side (top detectors).

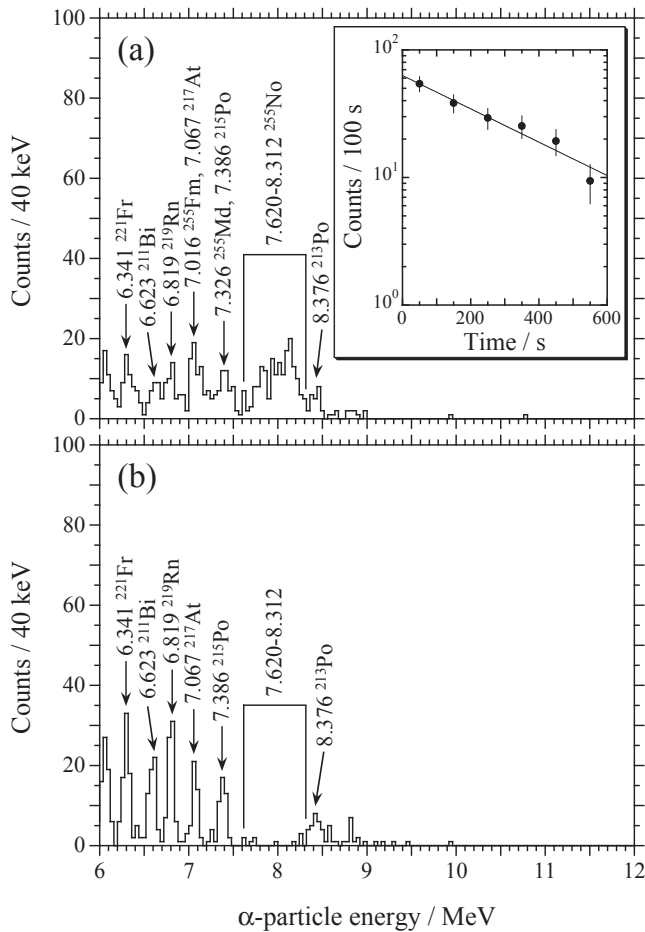


Figure 2. (a) α -Particle spectra measured in the 12-strip Si detector (SD) under the beam-off condition for 36000 s. The ^{22}Ne beam dose of 4.3×10^{17} was accumulated during the cycles of the beam-on (300 s) and beam-off (600 s) measurements. The magnetic rigidity of GARIS was set at 1.93 T m. The inset shows a decay curve of the 7.620–8.312-MeV α peaks of ^{255}No . (b) Background α -particle spectrum measured with SD for 82000 s before the beam experiment.

3. Results and Discussion

As mentioned in the previous section, no α peaks were identified in the α spectrum measured with SD under the beam-on condition (the total count rate of all strips of SD at > 1 MeV is about 2 k counts per second for the 1- μA beam intensity). Figure 2a shows a sum of α -particle spectra measured in all the strips of SD for 36000 s under the beam-off condition. The beam dose of 4.29×10^{17} was accumulated during the cycles of the beam-on (300 s) and beam-off (600 s) measurements. The magnetic rigidity of GARIS was 1.93 T m. As indicated in Figure 2a, α peaks of ^{255}No were identified in the energy region of interest ($E_\alpha = 7.620\text{--}8.312$ MeV),¹⁸ though many other α peaks are seen in the spectrum. Compared in Figure 2b is a background spectrum measured with SD for 82000 s before the beam experiment. Since SD was contaminated with long-lived ^{225}Ac ($T_{1/2} = 10.0$ d) and ^{227}Th ($T_{1/2} = 18.72$ d) which were implanted into SD as transfer reaction products from ^{232}Th in the previous experiment, α lines of their daughter nuclides of ^{221}Fr , ^{211}Bi , ^{219}Rn , ^{217}At , ^{215}Po , and ^{213}Po are clearly identified. Thus, the α peaks in Figure 2a except those for ^{255}No are unambiguously assigned as the background components, though small contributions of the daughter nuclides of ^{255}No , ^{255}Md ($T_{1/2} = 27$ min, $E_\alpha = 7.326$ MeV) and ^{255}Fm ($T_{1/2} = 20.07$ h, $E_\alpha = 7.016$ MeV), are seen in the spectrum. The decay curve of the 7.620–8.312 MeV α peaks of ^{255}No is shown in the inset of Figure 2a. The half-life of ^{255}No was determined to be 3.8 ± 0.7 min, which is in agreement with the literature value of 3.1 ± 0.2

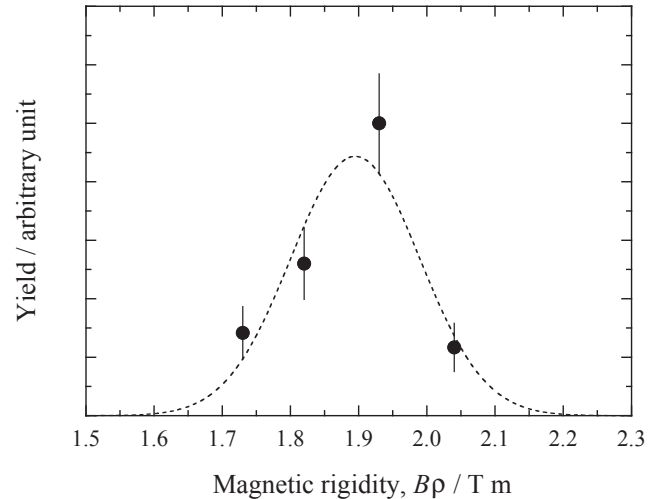


Figure 3. Yield variation of ^{255}No produced in the $^{238}\text{U}(^{22}\text{Ne}, 5n)^{255}\text{No}$ reaction as a function of the magnetic rigidity of GARIS. The dashed curve represents the result of the least-squares fitting with the Gaussian curve with a maximum yield at $B\rho = 1.89 \pm 0.02$ T m and a resolution of $\Delta B\rho/B\rho = 12 \pm 2\%$.

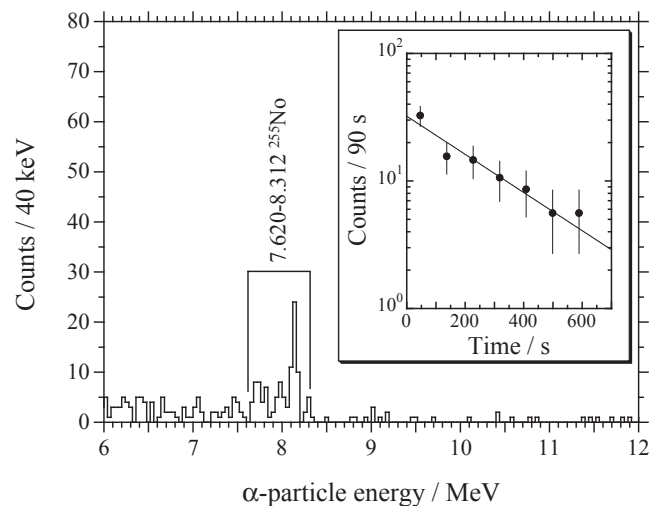


Figure 4. Sum of α -particle spectra measured in the seven top detectors of the rotating wheel apparatus MANON for 630 s after the 90-s aerosol collection. The 90-s aerosol collection was repeated 207 times. The beam dose of 2.8×10^{17} was accumulated. The helium flow rate was 1.0 L min^{-1} and the inner pressure of the gas-jet chamber was 38 kPa.

min.¹⁸ The decay curve also suggests that the contribution of 8.093-MeV α peak of ^{254}No ($T_{1/2} = 55$ s), which is producible in the $^{238}\text{U}(^{22}\text{Ne}, 6n)^{254}\text{No}$ reaction, is negligible within the error limit.

In Figure 3, relative yields of ^{255}No are shown as a function of the magnetic rigidity ($B\rho$) of the separator. As shown by a dashed curve in Figure 3, a least-squares fitting with the Gaussian curve gives a maximum yield at $B\rho = 1.89 \pm 0.02$ T m, where the transport efficiency of GARIS was evaluated to be about 5% for the focal plane of 60 mm diameter, assuming the cross section of the $^{238}\text{U}(^{22}\text{Ne}, 5n)^{255}\text{No}$ reaction to be 90 nb.¹⁴ The resolution of $\Delta B\rho/B\rho = 12 \pm 2\%$ suggests that the transport efficiency of GARIS would be increased by a factor of about 2 using the larger focal plane window of 100 mm diameter.

Figure 4 shows the sum of α -particle spectra measured in the seven top detectors of MANON. In this measurement, the beam dose of 2.81×10^{17} was accumulated. The 7.620–8.312-MeV α peaks of ^{255}No are clearly seen in the spectrum, indicating that the gas-jet transport of ^{255}No to MANON was successfully conducted after the physical separation with

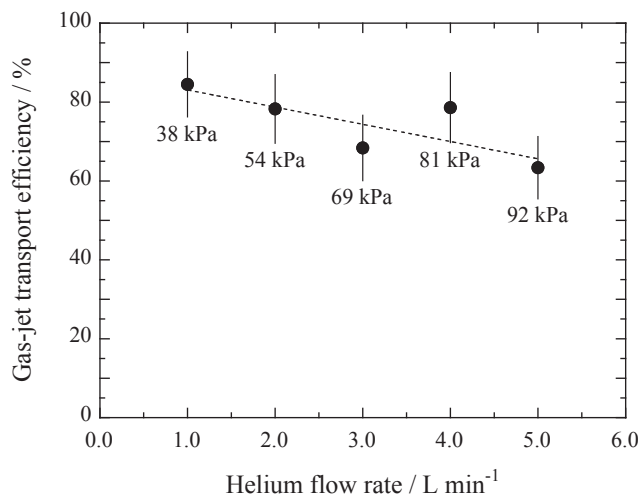


Figure 5. Variation of the gas-jet transport efficiency of ^{255}No as a function of the helium flow rate. The inner pressures of the gas-jet chamber are indicated for each data point.

GARIS. Background radioactivities such as ^{213}Po (8.376-MeV α) and $^{212\text{m}}\text{Po}$ (11.650-MeV α), which are largely produced in the transfer reactions on the lead impurity in the target,¹⁹ are fully removed by the present system. The decay curve for the 7.620–8.312-MeV component is shown in the inset of Figure 4a. The half-life was determined to be 3.4 ± 0.8 min. Since MANON was placed in the target room in this experiment, some background events caused by large amounts of neutrons during the irradiation are seen in the spectrum. Recently, we have constructed a chemistry laboratory, which is isolated with a 50-cm concrete shield from the target room, just behind the focal plane of GARIS. In the future, this kind of experiment will be conducted under improved background conditions.

In the conventional gas-jet system in that the beam passes in the target chamber, the gas-jet efficiency decreases due to the increasing plasma induced by the beam. As an example, we measured the gas-jet efficiencies of ^{173}W produced in the $^{154}\text{Gd}(^{22}\text{Ne}, xn)$ reaction without the beam separation by GARIS.¹⁴ It was found that the gas-jet efficiency of ^{173}W drastically decreases from 40% at 6.6 pA to 25% at 0.5 μA . In Figure 5, the gas-jet transport efficiencies of ^{255}No are shown as a function of the helium flow rate. In this work, the high gas-jet efficiencies of about 75% were achieved even at > 1 μA owing to the plasma-free condition. It is also found in Figure 5 that the gas-jet efficiencies are independent of the helium flow rate, i.e., the inner pressure of the gas-jet chamber, though a slight decreasing trend is seen. The recoil ranges of ^{255}No in helium at 38–90 kPa are calculated to be 16.0–6.6 mm, respectively, using the LISE++ code.²⁰ These recoil ranges are short enough as compared with the depth of the gas-jet chamber (60 mm). In our previous study,¹² the high gas-jet efficiencies of over 80% were obtained both for ^{206}Fr and ^{245}Fm . The recoil ranges of ^{206}Fr and ^{245}Fm in helium at 90 kPa were 30 and 18 mm, respectively. In the conventional gas-jet system, where a beam dump is placed in the bottom of the chamber, the gas is swept out through the capillary outlet to the vertical direction of the beam axis. Therefore, the position of the capillary outlet in the chamber should be exactly adjusted to the recoil ranges of the product nuclei to obtain their highest gas-jet yields. In the present system, the beam is separated with GARIS and hence we can put the capillary outlet in the bottom of the chamber (see Figure 1c). Thus, the gas is fed into the chamber through the four inlets directed to the surface of the Mylar window and is swept out thoroughly from the bottom of the chamber. This helium flow path in the gas-jet chamber would be advantageous to the range-independent gas-jet efficiencies. It is finally pointed out that the highest effi-

ciency of ^{255}No is achieved at the lowest chamber pressure of 38 kPa. This enables us to safely handle the thinner Mylar windows of < 1 μm thickness that should be required for SHE nuclides such as ^{261}Rf and ^{262}Db produced in the $^{248}\text{Cm}(^{18}\text{O}, 5n)^{261}\text{Rf}$ and $^{248}\text{Cm}(^{19}\text{F}, 5n)^{262}\text{Db}$ reactions, respectively.

4. Summary

We have successfully produced ^{255}No in the hot fusion reaction of $^{238}\text{U}(^{22}\text{Ne}, 5n)^{255}\text{No}$ using the gas-jet transport system coupled to GARIS. The α particles of ^{255}No separated with GARIS and transported by the gas-jet were clearly observed with a rotating wheel apparatus for α spectrometry. The high gas-jet efficiencies of about 75% were obtained at the beam intensities of over 1 μA , and they were independent of the recoil ranges of ^{255}No in the gas-jet chamber. These results suggest that the GARIS/gas-jet system is promising to explore new frontiers in SHE chemistry: (i) the background radioactivities originating from unwanted reaction products are strongly suppressed, (ii) the intense primary heavy-ion beam is absent in the gas-jet chamber and hence the high gas-jet efficiency is achieved, and (iii) the beam-free condition also makes it possible to investigate new chemical systems that were not accessible before. In the next phase, we plan to investigate the production of SHE nuclides with long half-lives for chemical experiments such as ^{261}Rf , ^{262}Db , ^{265}Sg , and ^{269}Hs based on the ^{248}Cm target.

Acknowledgement. The authors express their gratitude to the crew of the RIKEN Linear Accelerator for their invaluable assistance in the course of these experiments. This research was partially supported by the Ministry of Education, Science, Sports and Culture, Grant-in-Aid for Young Scientists (B), 16750055, 2004–2006 and (B), 17740179, 2005–2006.

References

- (1) M. Schädel, Ed. *The Chemistry of Superheavy Elements*, Kluwer Academic Publishers, Dordrecht, (2003).
- (2) M. Schädel, *Angew. Chem. Int. Ed.* **45**, 368 (2006).
- (3) R. Eichler, N. V. Aksenov, A. V. Belozarov, G. A. Bozhikov, V. I. Chepigin, S. N. Dmitriev, R. Dressler, H. W. Gäggeler, V. A. Gorshkov, F. Haenssler, M. G. Itkis, A. Laube, V. Ya. Lebedev, O. N. Malyshev, Yu. Ts. Oganessian, O. V. Petrushkin, D. Piguet, P. Rasmussen, S. V. Shishkin, A. V. Shutov, A. I. Svirikhin, E. E. Tereshatov, G. K. Vostokin, M. Wegrzecki, and A. V. Yerebin, *Nature* **447**, 72 (2007).
- (4) Ch. E. Düllmann, *Eur. Phys. J. D* **45**, 75 (2007).
- (5) J. P. Omtvedt, J. Alstad, H. Breivik, J. E. Dyve, K. Eberhardt, C. M. Folden III, T. Ginter, K. E. Gregorich, E. A. Hult, M. Johansson, U. W. Kirbach, D. M. Lee, M. Mendel, A. Nähler, V. Ninov, L. A. Omtvedt, J. B. Patin, G. Skarnemark, L. Stavsetra, R. Sudowe, N. Wiehl, B. Wierczinski, P. A. Wilk, P. M. Zielinski, J. V. Kratz, N. Trautmann, H. Nitsche, and D. C. Hoffman, *J. Nucl. Radiochem. Sci.* **3**, 121 (2002).
- (6) L. Stavsetra, K. E. Gregorich, J. Alstad, H. Breivik, K. Eberhardt, C. M. Folden III, T. N. Ginter, M. Johansson, U. W. Kirbach, D. M. Lee, M. Mendel, L. A. Omtvedt, J. B. Patin, G. Skarnemark, R. Sudowe, P. A. Wilk, P. M. Zielinski, H. Nitsche, D. C. Hoffman, and J. P. Omtvedt, *Nucl. Instrum. Methods A* **543**, 509 (2005).
- (7) Ch. E. Düllmann, G. K. Pang, C. M. Folden III, K. E. Gregorich, D. C. Hoffman, H. Nitsche, R. Sudowe, and P. M. Zielinski, *Advances in Nuclear and Radiochemistry, General and Interdisciplinary, Vol. 3*, Eds. S. M. Qaim and H. H. Coenen, Forschungszentrum Jülich GmbH, Jülich, (2004), p 147.
- (8) Ch. E. Düllmann, C. M. Folden III, K. E. Gregorich, D. C.

- Hoffman, D. Leitner, G. K. Pang, R. Sudowe, P. M. Zielinski, and H. Nitsche, *Nucl. Instrum. Methods A* **551**, 528 (2005).
- (9) R. Sudowe, M. G. Galvert, Ch. E. Düllmann, L. M. Farina, C. M. Folden III, K. E. Gregorich, S. E. H. Gallaher, D. C. Hoffman, S. L. Nelson, D. C. Phillips, J. M. Schwantes, R. E. Wilson, P. M. Zielinski, and H. Nitsche, *Radiochim. Acta* **94**, 123 (2006).
- (10) U. W. Kirbach, C. M. Folden III, T. N. Ginter, K. E. Gregorich, D. M. Lee, V. Ninov, J. P. Omtvedt, J. B. Patin, N. K. Seward, D. A. Strellis, R. Sudowe, A. Türler, P. A. Wilk, P. M. Zielinski, D. C. Hoffman, and H. Nitsche, *Nucl. Instrum. Methods A* **484**, 587 (2002).
- (11) M. Schädel, *J. Nucl. Radiochem. Sci.* **8**, 47 (2007).
- (12) H. Haba, D. Kaji, H. Kikunaga, T. Akiyama, N. Sato, K. Morimoto, A. Yoneda, K. Morita, T. Takabe, and A. Shinohara, *J. Nucl. Radiochem. Sci.* **8**, 55 (2007).
- (13) H. Kikunaga, H. Haba, D. Kaji, and K. Morita, *RIKEN Accel. Prog. Rep.* **41** (in press).
- (14) H. Haba, T. Akiyama, D. Kaji, H. Kikunaga, T. Kuribayashi, K. Morimoto, K. Morita, K. Ooe, N. Sato, A. Shinohara, T. Takabe, Y. Tashiro, A. Toyoshima, A. Yoneda, and T. Yoshimura, *Eur. Phys. J. D* **45**, 81 (2007).
- (15) K. Morita, K. Morimoto, D. Kaji, H. Haba, E. Ideguchi, R. Kanungo, K. Katori, H. Koura, H. Kudo, T. Ohnishi, A. Ozawa, T. Suda, K. Sueki, I. Tanihata, H. Xu, A. V. Yeremin, A. Yoneda, A. Yoshida, Y.-L. Zhao, and T. Zhen, *Eur. Phys. J. A* **21**, 257 (2004).
- (16) J. F. Ziegler, *The Stopping and Range of Ions in Matter, SRIM* (<http://www.srim.org/>).
- (17) Y. Nagame, M. Asai, H. Haba, S. Goto, K. Tsukada, I. Nishinaka, K. Nishio, S. Ichikawa, A. Toyoshima, K. Akiyama, H. Nakahara, M. Sakama, M. Schädel, J. V. Kratz, H. W. Gäggeler, and A. Türler, *J. Nucl. Radiochem. Sci.* **3**, 85 (2002).
- (18) R. B. Firestone and V. S. Shirley, *Table of Isotopes, 8th ed.* John Wiley & Sons, New York, (1996).
- (19) G. N. Flerov, G. N. Akap'ev, A. G. Demin, V. A. Druin, Yu. V. Lobanov, and B. V. Fefilov, *Sov. J. Nucl. Phys.* **7**, 588 (1968).
- (20) O. B. Tarasov and D. Bazin, *LISE++* (<http://groups.nslc.msu.edu/lise/>).

